

# Modelling of cyclist’s power for timetrials on a velodrome

Len Bos\*, Michael A. Slawinski†, Raphaël A. Slawinski‡, Theodore Stanoev§

## Abstract

We formulate a phenomenological model to study the power applied by a cyclist on a velodrome—for individual timetrials—taking into account the straights, circular arcs, connecting transition curves, and banking. The dissipative forces we consider are air resistance, rolling resistance, lateral friction and drivetrain resistance. Also, in general, the power is used to increase the kinetic and potential energy. However, to model a steady ride—as expected for individual timetrials—we assume a constant centre-of-mass speed and allow the cadence and power to vary during a lap. Hence, the only mechanical energy to consider is the increase of potential energy due to raising the centre of mass upon exiting each curve. Following derivations and justifications of expressions that constitute this mathematical model, we present a numerical example. We show that, as expected, the cadence and power vary only slightly during a steady ride. Also, we examine changes in the required average power per lap due to modifications of various quantities, such as air density at a velodrome, laptime and several others, as well as the model sensitivity to input errors. Such an examination is of immediate use in strategizing the performance for individual pursuits and the Hour Record, as well as in evaluating the reliability of model predictions.

## 1 Introduction

In this article, we formulate a mathematical model to examine the power expended by a cyclist on a velodrome. Our assumptions limit the model to individual time trials; we do not include drafting effects, which arise in team pursuits. Furthermore, our model does not account for the initial acceleration; we assume the cyclist to be already in a launched effort, which renders the model adequate for longer events, such as a 4000-metre pursuit or, in particular, the Hour Record.

Geometrically, we consider a velodrome with its straights, circular arcs and connecting transition curves, whose inclusion — as indicated by Fitzgerald et al. (2021) — has been commonly neglected in previous studies. While this inclusion presents a mathematical challenge, it increases the empirical adequacy of the model.

Various power models and velodrome geometries have been presented in previous studies. Almost a quarter-of-a-century ago, Martin et al. (1998) formulate and examine a road-cycling model. Proceeding with velodrome models, Underwood and Jermy (2010, 2014) formulate and examine a model for individual pursuits that includes leaning on the bends, but only use straights and bends without transition curves. Lukes et al. (2012) model the power of a cyclist on a velodrome, including the tire scrubbing effects. Fitton and Symons (2018) present a model that includes slip and steering angles for deviations of the bicycle wheels from the black line, and use velodrome models based on a theodolite measurements.

\*Università di Verona, Italy, [leonardpeter.bos@univr.it](mailto:leonardpeter.bos@univr.it)

†Memorial University of Newfoundland, Canada, [msslawins@mac.com](mailto:msslawins@mac.com)

‡Mount Royal University, Canada, [rslawinski@mtroyal.ca](mailto:rslawinski@mtroyal.ca)

§Memorial University of Newfoundland, Canada, [theodore.stanoev@gmail.com](mailto:theodore.stanoev@gmail.com)

Most recently, Fitzgerald et al. (2021) quantify the effects of transition curves on a power model consistent with Lukes et al. (2012) and Martin et al. (1998). They consider two types of transition curves, namely, a twice-differentiable linear increase in curvature, which is the Euler spiral, and a sinusoid, which exhibits a continuous derivative of curvature. The effects of these curves are estimated using least squares optimization of black-line measurements obtained with theodolite measurements.

We begin this article by expressing mathematically the geometry of both the black line and the inclination of the track. We provide a detailed derivation of the Euler spiral, which appeared as a preprint and was referred to by Fitzgerald et al. (2021) as the most detailed to date. Also, we derive a Bloss-transition curve, whose curvature is thrice-differentiable. Our expressions are accurate representations of the common geometry of modern 250-metre velodromes, whose design details were provided by Mehdi Kordi (*pers. comm.*, 2020). We proceed to formulate an expression for power used against dissipative forces and power used to increase mechanical energy. In particular, while earlier work considers changes in potential energy as a function of vertical location on a banked velodrome (e.g., Benham et al. (2020)) or of the lean angle and the vertical inclination of trajectory (e.g., Fitton and Symons (2018)), we consider — in accordance with the assumption of instantaneous rotational equilibrium — increases in potential energy due solely to straightening of the cyclist upon exiting the curves, with wheels remaining along the black line. We show that a significant amount of power is expended in that process. To present a numerical example and for a comparison with the model of Fitzgerald et al. (2021), we examine the case of a constant centre-of-mass speed, which we consider the best mathematical analogy for steadiness of timetrial efforts on a velodrome. We complete the article with conclusions. In appendices, we present derivations of expressions for the air resistance and lean angle.

## 2 Track

### 2.1 Black-line parameterization

To model the required power of a cyclist who follows the black line, in a constant aerodynamic position, as illustrated in Figure 1, we define this line by three parameters.

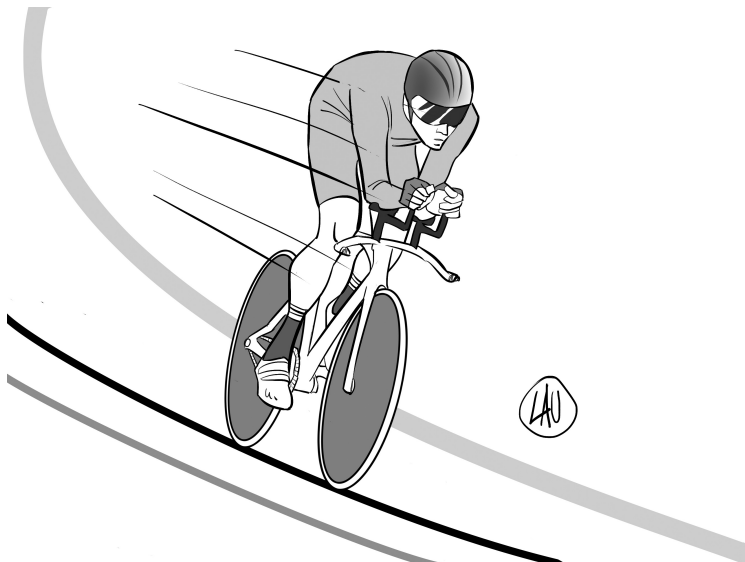


**Figure 1:** A constant aerodynamic position along the black line

- $L_s$ : the half-length of the straight
- $L_t$ : the length of the transition curve between the straight and the circular arc
- $L_a$ : the length of the remainder of the quarter circular arc

The length of the track is  $S = 4(L_s + L_t + L_a)$ . In Figure 2, we show a quarter of a black line for  $L_s = 19$  m,  $L_t = 13.5$  m and  $L_a = 30$  m, which results in  $S = 250$  m. This curve has continuous

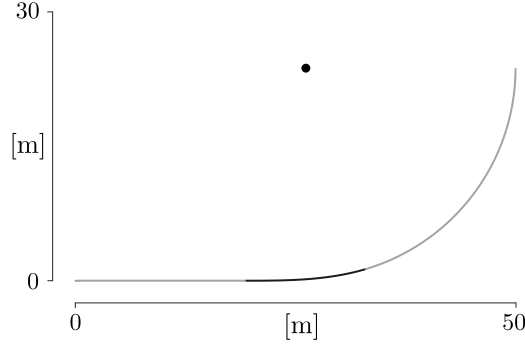


**Figure 2:** A quarter of the black line for a 250-metre track

derivative up to order two; it is a  $C^2$  curve, whose curvature is continuous.

To formulate, in Cartesian coordinates, the curve shown in Figure 2, we consider the following.

- The straight,

$$y_1 = 0, \quad 0 \leq x \leq a,$$

shown in gray, where  $a := L_s$ .

- The transition, shown in black — following a standard design practice — we take to be an Euler spiral, which can be parameterized by Fresnel integrals,

$$x_2(\varsigma) = a + \sqrt{\frac{2}{A}} \int_0^{\varsigma\sqrt{\frac{A}{2}}} \cos(x^2) dx \quad \text{and} \quad y_2(\varsigma) = \sqrt{\frac{2}{A}} \int_0^{\varsigma\sqrt{\frac{A}{2}}} \sin(x^2) dx,$$

with  $A > 0$  to be determined; herein,  $\varsigma$  is the curve parameter. Since the arclength differential,  $ds$ , is such that

$$ds = \sqrt{x_2'(\varsigma)^2 + y_2'(\varsigma)^2} d\varsigma = \sqrt{\cos^2\left(\frac{A\varsigma^2}{2}\right) + \sin^2\left(\frac{A\varsigma^2}{2}\right)} d\varsigma = d\varsigma,$$

we write the transition curve as

$$(x_2(s), y_2(s)), \quad 0 \leq s \leq b := L_t.$$

- The circular arc, shown in gray, whose centre is  $(c_1, c_2)$  and whose radius is  $R$ , with  $c_1$ ,  $c_2$  and  $R$  to be determined. Since its arclength is specified to be  $c := L_a$ , we may parameterize the quarter circle by

$$x_3(\theta) = c_1 + R \cos(\theta) \tag{1}$$

and

$$y_3(\theta) = c_2 + R \sin(\theta), \tag{2}$$

where  $-\theta_0 \leq \theta \leq 0$ , for  $\theta_0 := c/R$ . The centre of the circle is shown as a black dot in Figure 2.

We wish to connect these three curve segments so that the resulting global curve is continuous along with its first and second derivatives. This ensures that the curvature of the track is also continuous.

To do so, let us consider the connection between the straight and the Euler spiral. Herein,  $x_2(0) = a$  and  $y_2(0) = 0$ , so the spiral connects continuously to the end of the straight at  $(a, 0)$ . Also, at  $(a, 0)$ ,

$$\frac{dy}{dx} = \frac{y_2'(0)}{x_2'(0)} = \frac{0}{1} = 0,$$

which matches the derivative of the straight line. Furthermore, the second derivatives match, since

$$\frac{d^2y}{dx^2} = \frac{y_2''(0)x_2'(0) - y_2'(0)x_2''(0)}{(x_2'(0))^2} = 0,$$

which follows, for any  $A > 0$ , from

$$x_2'(\varsigma) = \cos^2\left(\frac{A\varsigma^2}{2}\right), \quad y_2'(\varsigma) = \sin^2\left(\frac{A\varsigma^2}{2}\right) \quad (3)$$

and

$$x_2''(\varsigma) = -A\varsigma \sin\left(\frac{A\varsigma^2}{2}\right), \quad y_2''(\varsigma) = A\varsigma \cos\left(\frac{A\varsigma^2}{2}\right).$$

Let us consider the connection between the Euler spiral and the arc of the circle. In order that these connect continuously,

$$(x_2(b), y_2(b)) = (x_3(-\theta_0), y_3(-\theta_0)),$$

we require

$$x_2(b) = c_1 + R \cos(\theta_0) \iff c_1 = x_2(b) - R \cos\left(\frac{c}{R}\right) \quad (4)$$

and

$$y_2(b) = c_2 - R \sin(\theta_0) \iff c_2 = y_2(b) + R \sin\left(\frac{c}{R}\right). \quad (5)$$

For the tangents to connect continuously, we invoke expression (3) to write

$$(x_2'(b), y_2'(b)) = \left(\cos\left(\frac{Ab^2}{2}\right), \sin\left(\frac{Ab^2}{2}\right)\right).$$

Following expressions (1) and (2), we obtain

$$(x_3'(-\theta_0), y_3'(-\theta_0)) = (R \sin(\theta_0), R \cos(\theta_0)),$$

respectively. Matching the unit tangent vectors results in

$$\cos\left(\frac{Ab^2}{2}\right) = \sin\left(\frac{c}{R}\right), \quad \sin\left(\frac{Ab^2}{2}\right) = \cos\left(\frac{c}{R}\right). \quad (6)$$

For the second derivative, it is equivalent—and easier—to match the curvature. For the Euler spiral,

$$\kappa_2(s) = \frac{x_2'(s)y_2''(s) - y_2'(s)x_2''(s)}{\left((x_2'(s))^2 + (y_2'(s))^2\right)^{\frac{3}{2}}} = As \cos^2\left(\frac{As^2}{2}\right) + As \sin^2\left(\frac{As^2}{2}\right) = As,$$

which is indeed the defining characteristic of an Euler spiral: the curvature grows linearly in the arclength. Hence, to match the curvature of the circle at the connection, we require

$$Ab = \frac{1}{R} \iff A = \frac{1}{bR}.$$

Substituting this value of  $A$  in equations (6), we obtain

$$\begin{aligned}\cos\left(\frac{b}{2R}\right) &= \sin\left(\frac{c}{R}\right), & \sin\left(\frac{b}{2R}\right) &= \cos\left(\frac{c}{R}\right) \\ \iff \frac{b}{2R} &= \frac{\pi}{2} - \frac{c}{R} \\ \iff R &= \frac{b+2c}{\pi}.\end{aligned}$$

It follows that

$$A = \frac{1}{bR} = \frac{\pi}{b(b+2c)};$$

hence, the continuity condition stated in expressions (4) and (5) determines the centre of the circle,  $(c_1, c_2)$ .

For the case shown in Figure 2, the numerical values are  $A = 3.1661 \times 10^{-3} \text{ m}^{-2}$ ,  $R = 23.3958 \text{ m}$ ,  $c_1 = 25.7313 \text{ m}$  and  $c_2 = 23.7194 \text{ m}$ . The complete track — with its centre at the origin,  $(0, 0)$  — is shown in Figure 3. The corresponding track curvature is shown in Figure 4. Note that the curvature

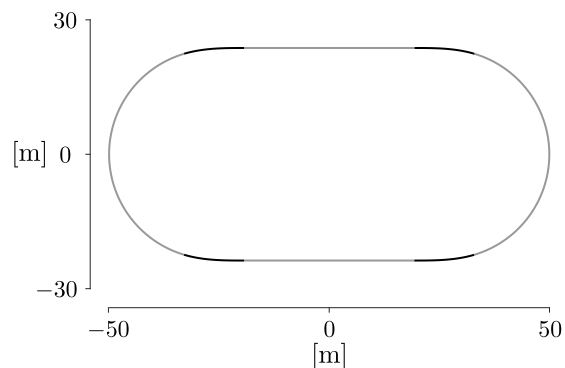


**Figure 3:** Black line of 250-metre track

transitions linearly from the constant value of straight,  $\kappa = 0$ , to the constant value of the circular arc,  $\kappa = 1/R$ .

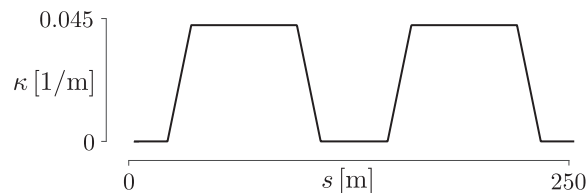


**Figure 4:** Curvature of the black line,  $\kappa$ , as a function of distance,  $s$ , with a linear transition between the zero curvature of the straight and the  $1/R$  curvature of the circular arc

## 2.2 $C^3$ transition curve

As stated by Fitzgerald et al. (2021),

[t]here can be a trade-off between good spatial fit (low continuity for matching a built velodrome) and a good physical fit (high continuity for matching a cyclist's path). If this

model is used to calculate the motion of cyclists on a velodrome surface then a spatial fit can be prioritised. However, if it is used to directly model the path of a cyclist then higher continuity is required.

Should it be desired that the trajectory have continuous derivatives up to order  $r \geq 0$ —which makes it in class  $C^r$ , so that its curvature is of class  $C^{r-2}$ —it is possible to achieve this by a transition curve  $y = p(x)$ , where  $p(x)$  is a polynomial of degree  $2r - 1$  and the solution of a  $4 \times 4$  system of nonlinear equations, assuming a solution exists.

In case  $r = 2$ , this would correspond to a transition by a polynomial of degree  $2r - 1 = 3$ , often referred to as a cubic spiral. In case  $r = 3$ , this would correspond to a transition by a polynomial of degree  $2r - 1 = 5$ , often referred to as a Bloss transition.

To see how to do this, for simplicity's sake, let  $a = L_s$ . We use a Cartesian formulation, namely,

- $y = 0, 0 \leq x \leq a$ : the halfstraight
- $y = p(x), a \leq x \leq X$ : the transition curve between the straight and circular arc
- $y = c_2 - \sqrt{R^2 - (x - c_1)^2}$ : the end circle, with centre at  $(c_1, c_2)$  and radius  $R$ .

Here  $x = X$  is the point at which the polynomial transition connects to the circle  $(x - c_1)^2 + (y - c_2)^2 = R^2$ .

$X, c_1, c_2$  and  $R$  are *a priori* unknowns that need to be determined. These four values determine completely the transition zone,  $y = p(x), a \leq x \leq X$ .

Given  $X, c_1, c_2$  and  $R$ , we can compute  $p(x)$  as the Lagrange-Hermite interpolant of the data

$$p^{(j)}(a) = 0, \quad 0 \leq j \leq r, \quad \text{and} \quad p^{(j)}(X) = y^{(j)}(X), \quad 0 \leq j \leq r,$$

where  $y(x) = c_2 - \sqrt{R^2 - (x - c_1)^2}$  is the circle. Indeed, this is given in Newton form as

$$p(x) = \sum_{j=0}^{2r+1} p[x_0, \dots, x_j] \prod_{k=0}^{j-1} (x - x_k),$$

with

$$x_0 = x_1 = \dots = x_r = a \quad \text{and} \quad x_{r+1} = \dots = x_{2r+1} = X$$

and, for any values  $t_1, t_2, \dots, t_m$ , the divided difference,

$$p[t_1, t_2, \dots, t_m],$$

may be computed from the recurrence

$$p[t_1, \dots, t_m] = \frac{p[t_2, \dots, t_m] - p[t_1, \dots, t_{m-1}]}{t_m - t_1},$$

with

$$p \underbrace{[a, \dots, a]}_{\text{multiplicity } j+1} := 0, \quad 0 \leq j \leq r$$

and

$$p \underbrace{[X, \dots, X]}_{\text{multiplicity } j+1} := \frac{y^{(j)}(X)}{j!}, \quad 0 \leq j \leq r,$$

where again  $y(x) = c_2 - \sqrt{R^2 - (x - c_1)^2}$  is the circle.

Note, however, that this defines  $p(x)$  as a polynomial of degree  $2r + 1$  exceeding our claimed degree  $2r - 1$  by 2. Hence, the first two of our equations are that  $p(x)$  is actually of degree  $2r - 1$ , i.e., its two leading coefficients are zero. More specifically, from the Newton form,

$$p[\underbrace{a, a, \dots, a}_{r+1 \text{ copies}}, \underbrace{X, X, \dots, X}_{r+1 \text{ copies}}] = 0 \quad (7)$$

and

$$p[\underbrace{a, a, \dots, a}_{r+1 \text{ copies}}, \underbrace{X, X, \dots, X}_r] = 0. \quad (8)$$

The third equation is that the length of the transition is specified to be  $L_t$ , i.e.,

$$\int_a^X \sqrt{1 + (p'(x))^2} dx = L_t. \quad (9)$$

Note that this integral has to be estimated numerically.

Finally, the fourth equation is that the remainder of the circular arc—from  $x = X$  to the apex  $x = c_1 + R$ —have length  $L_a$ . This is equally accomplished. The two endpoints of the circular arc are  $(X, y(X))$  and  $(c_1 + R, c_2)$  giving a circular segment of angle  $\theta$ , say, between the two vectors connecting these points to the centre, i.e.,  $\langle X - c_1, y(X) - c_2 \rangle$  and  $\langle R, 0 \rangle$ . Then,

$$\cos(\theta) = \frac{\langle X - c_1, y(X) - c_2 \rangle \cdot \langle R, 0 \rangle}{\|\langle X - c_1, y(X) - c_2 \rangle\|_2 \|\langle R, 0 \rangle\|_2} = \frac{X - c_1}{R}.$$

Hence the fourth equation is

$$R \cos^{-1} \left( \frac{X - c_1}{R} \right) = L_a. \quad (10)$$

Together, equations (7), (8), (9) and (10) form a system of four nonlinear equations in four unknowns,  $c_1$ ,  $c_2$ ,  $R$  and  $X$ , determining a  $C^r$  transition given by  $p(x)$ , a polynomial of degree  $2r - 1$ , satisfying the design parameters.

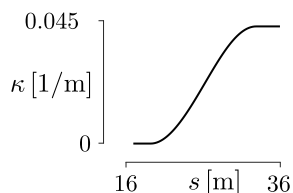


**Figure 5:** Transition zone track curvature,  $\kappa$ , as a function of distance,  $s$ , which—in contrast to Figure 4—exhibits a smooth ( $C^1$ ) transition between the zero curvature of the straight and the  $1/R$  curvature of the circular arc

For the velodrome under consideration, and a Bloss  $C^3$  transition, with curvature  $C^1$ , we obtain  $c_1 = 25.7565$  m,  $c_2 = 23.5753$  m,  $R = 23.3863$  m and  $X = 32.3988$  m, which—as expected—are similar to values obtained in Section 2.1. The corresponding trajectory curvature is shown in Figure 5.

Returning to the quote on page 5, the requirement of differentiability of the trajectory traced by bicycle wheels, which is expressed in spatial coordinates, is a consequence of a dynamic behaviour, which is expressed in temporal coordinates, namely, the requirement of smoothness of the derivative of acceleration, which is commonly referred to as a jolt. In other words, a natural motion of the bicycle-cyclist system, which is laterally unconstrained, ensures that the third temporal derivative of position is smooth; the black line smoothed by this motion.

### 2.3 Track-inclination angle

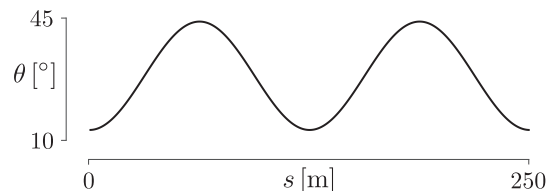


**Figure 6:** Track inclination,  $\theta$ , as a function of the black-line distance,  $s$

There are many possibilities to model the track inclination angle. We choose a trigonometric formula in terms of arclength, which is a good analogy of an actual 250-metre velodrome. The minimum inclination of  $13^\circ$  corresponds to the midpoint of the straight, and the maximum of  $44^\circ$  to the apex of the circular arc. For a track of length  $S$ ,

$$\theta(s) = 28.5 - 15.5 \cos\left(\frac{4\pi}{S}s\right); \quad (11)$$

$s = 0$  refers to the midpoint of the lower straight, in Figure 3, and the track is oriented in the counterclockwise direction. Figure 6 shows this inclination for  $S = 250$  m.

It is not uncommon for tracks to be slightly asymmetric with respect to the inclination angle. In such a case, they exhibit a rotational symmetry by  $\pi$ , but not a reflection symmetry about the vertical or horizontal axis. This asymmetry can be modeled by including  $s_0$  in the argument of the cosine in expression (11).

$$\theta(s) = 28.5 - 15.5 \cos\left(\frac{4\pi}{S}(s - s_0)\right); \quad (12)$$

$s_0 \approx 5$  provides a good model for several existing velodromes. Referring to discussions about the London Velodrome of the 2012 Olympics, Solarczyk (2020) writes that

the slope of the track going into and out of the turns is not the same. This is simply because you always cycle the same way around the track, and you go shallower into the turn and steeper out of it.

The last statement is not obvious. For a constant centre-of-mass speed, under rotational equilibrium, the same transition curves along the black line imply the same lean angle.

## 3 Dissipative forces

A mathematical model to account for the power required to propel a bicycle against dissipative forces is based on

$$P_F = FV, \quad (13)$$

where  $F$  stands for the magnitude of forces opposing the motion and  $V$  for speed. Herein, we model the rider as undergoing instantaneous circular motion, in rotational equilibrium about the line of contact of the tires with the ground. In view of Figure 7, along the black line, in windless conditions,



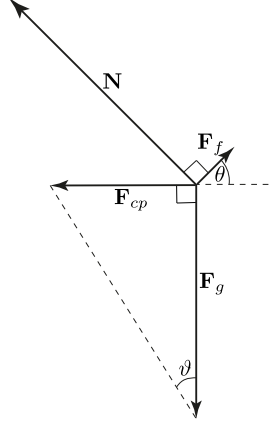


**Figure 7:** Force diagram: Inertial frame

$$P_F = \frac{1}{1 - \lambda} \left\{ \right. \quad (14a)$$

$$\left( C_{rr} \underbrace{\overbrace{m g (\sin \theta \tan \vartheta + \cos \theta)}^N} \cos \theta + C_{sr} \left| \underbrace{\overbrace{m g \frac{\sin(\theta - \vartheta)}{\cos \vartheta}}^{F_f}} \right| \sin \theta \right) v \quad (14b)$$

$$\left. + \frac{1}{2} C_d A \rho V^3 \right\}, \quad (14c)$$

where  $m$  is the mass of the cyclist and the bicycle,  $g$  is the acceleration due to gravity,  $\theta$  is the track-inclination angle,  $\vartheta$  is the bicycle-cyclist lean angle,  $C_{rr}$  is the rolling-resistance coefficient,  $C_{sr}$  is the coefficient of the lateral friction,  $C_d A$  is the air-resistance coefficient,  $\rho$  is the air density,  $\lambda$  is the drivetrain-resistance coefficient. Herein,  $v$  is the speed at which the contact point of the rotating wheels moves along the track, which we assume to coincide with the black-line speed.  $V$  is the centre-of-mass speed. Since lateral friction is a dissipative force, it does negative work, and the work done against it — as well as the power — are positive. For this reason, in expression (14b), we consider the magnitude,  $|\cdot|$ .

To formulate summand (14b), we use the relations among the magnitudes of vectors  $\mathbf{N}$ ,  $\mathbf{F}_g$ ,  $\mathbf{F}_{cp}$  and  $\mathbf{F}_f$ , illustrated in Figure 7. In accordance with Newton's second law, for a cyclist to maintain a horizontal trajectory, the resultant of all vertical forces must be zero,

$$\sum F_y = 0 = N \cos \theta + F_f \sin \theta - F_g. \quad (15)$$

In other words,  $\mathbf{F}_g$  must be balanced by the sum of the vertical components of normal force,  $\mathbf{N}$ , and the friction force,  $\mathbf{F}_f$ , which is parallel to the velodrome surface and perpendicular to the instantaneous velocity. Depending on the centre-of-mass speed and the radius of curvature for the centre-of-mass trajectory, if  $\vartheta < \theta$ ,  $\mathbf{F}_f$  points upwards, in Figure 7, which corresponds to its pointing outwards, on the velodrome; if  $\vartheta > \theta$ , it points downwards and inwards. If  $\vartheta = \theta$ ,  $\mathbf{F}_f = \mathbf{0}$ . Since we assume no lateral motion,  $\mathbf{F}_f$  accounts for the force that prevents it. Heuristically, it can be conceptualized as the force exerted in a lateral deformation of the tires.

For a cyclist to follow the curved bank, the resultant of the horizontal forces,

$$\sum F_x = -N \sin \theta + F_f \cos \theta = -F_{cp}, \quad (16)$$

is the centripetal force,  $\mathbf{F}_{cp}$ , whose direction is perpendicular to the direction of motion and points towards the centre of the radius of curvature. According to the rotational equilibrium about the centre of mass,

$$\sum \tau_z = 0 = F_f h \cos(\theta - \vartheta) - N h \sin(\theta - \vartheta), \quad (17)$$

where  $\tau_z$  is the torque about the axis parallel to the instantaneous velocity, which implies

$$F_f = N \tan(\theta - \vartheta). \quad (18)$$

Substituting expression (18) in expression (15), we obtain

$$N = \frac{m g}{\cos \theta - \tan(\theta - \vartheta) \sin \theta} = m g (\sin \theta \tan \vartheta + \cos \theta). \quad (19)$$

Using this result in expression (18), we obtain

$$F_f = m g (\sin \theta \tan \vartheta + \cos \theta) \tan(\theta - \vartheta) = m g \frac{\sin(\theta - \vartheta)}{\cos \vartheta}. \quad (20)$$

Since the lateral friction,  $\mathbf{F}_f$ , is a dissipative force, it does negative work. Hence, the work done against it—as well as the power—needs to be positive. For this reason, in expression (14b), we consider the magnitude of  $\mathbf{F}_f$ .

For summand (14c), a formulation of  $C_d A \rho V^2/2$ , therein, which we denote by  $F_a$ , is discussed in Appendix A.

We restrict our study to steady efforts, which—following the initial acceleration—are consistent with a pace of an individual pursuit or the Hour Record. Steadiness of effort is an important consideration in the context of measurements within a fixed-wheel drivetrain, as discussed by Danek et al. (2021, Section 5.2).<sup>1</sup> For road-cycling models (e.g., Danek et al., 2021, expression (1))—where curves are neglected and there is no need to distinguish between the wheel speed and the centre-of-mass speed—such a restriction would correspond to setting the acceleration,  $a$ , to zero. On a velodrome, this is tantamount to a constant centre-of-mass speed,  $dV/dt = 0$ .

Let us return to expression (14). Therein,  $\theta$  is given by expression (11). As shown in Appendix B, the lean angle is

$$\vartheta = \arctan \frac{V^2}{g r_{\text{CoM}}}, \quad (21)$$

where  $r_{\text{CoM}}$  is the centre-of-mass radius, and—along the curves, at any instant—the centre-of-mass speed is

$$V = v \frac{\overbrace{(R - h \sin \vartheta)}^{r_{\text{CoM}}}}{R} = v \left( 1 - \frac{h \sin \vartheta}{R} \right), \quad (22)$$

where  $R$  is the radius discussed in Section 2.1 and  $h$  is the centre-of-mass height of the bicycle-cyclist system at  $\vartheta = 0$ . Along the straights, the black-line speed is equal to the centre-of-mass speed,  $v = V$ . As expected,  $V = v$  if  $h = 0$ ,  $\vartheta = 0$  or  $R = \infty$ . The lean angle,  $\vartheta$ , is determined by

<sup>1</sup>For a fixed-wheel drivetrain, the momentum of a bicycle-cyclist system results in rotation of pedals even without any force applied by a cyclist. For variable efforts, this leads to inaccuracy of measurements of the instantaneous power generated by a cyclist.

assuming that, at all times, the system is in rotational equilibrium about the line of contact of the tires with the ground; this assumption yields the implicit condition on  $\vartheta$ , stated in expression (21).

As illustrated in Figure 7, expressions (21) and (22) assume instantaneous circular motion of the centre of mass to occur in a horizontal plane. Therefore, using these expression implies neglecting the vertical motion of the centre of mass. Accounting for the vertical motion of the centre of mass would mean allowing for a nonhorizontal centripetal force, and including the work done in raising the centre of mass.

In our model, we also neglect the effect of air resistance of rotating wheels (e.g., Danek et al., 2021, Section 5.5). We consider only the air resistance due to the translational motion of the bicycle-cyclist system.

## 4 Conservative forces

### 4.1 Mechanical energy

Commonly, in road-cycling models (e.g., Danek et al., 2021, expression (1)), we include  $mg \sin \Theta$ , where  $\Theta$  corresponds to a slope; this term represents force due to changes in potential energy associated with hills. This term is not included in expression (14). However—even though a black-line of a velodrome is horizontal—we need to account for the power required to increase potential energy to raise the centre of mass upon exiting the curves.

In Section 3, we assume the cyclist’s centre of mass to travel in a horizontal plane. This is a simplification, since the centre of mass follows a three-dimensional trajectory, lowering while entering a turn and rising while exiting it. We cannot use the foregoing assumption to calculate—from first principles—the change in the cyclist’s potential energy, even though this approach allows us to calculate the power expended against dissipative forces, which is dominated by the power expended against air resistance, which is proportional to the cube of the centre-of-mass speed,  $V$ . Along the transition curves,  $\mathbf{V}$  has both horizontal and vertical components, and we are effectively neglecting the latter. The justification for doing so—in Section 3—is that the magnitude of the horizontal component, corresponding to the cyclist’s forward motion, is much larger than that of the vertical component, corresponding to the up and down motion of the centre of mass. In Section 4.3, below, we calculate the change in the cyclist’s potential energy instead using the change in the lean angle, whose values are obtained from the assumption of instantaneous rotational equilibrium

Since dissipative forces, discussed in Section 3, are nonconservative, the average power expended against them depends on the details of the path traveled by the cyclist, not just on its endpoints. For this reason, to calculate the average power expended against dissipative forces, we require a detailed model of the cyclist’s path to calculate the instantaneous power. Instantaneous power is averaged to obtain the average power expended against dissipative forces over a lap. This is not the case for calculating the average power needed to increase the cyclist’s mechanical energy. Provided this increase is monotonic, the change in mechanical energy—and therefore the average power—does not depend on the details of the path traveled by the cyclist, but only on its endpoints. In brief, the path dependence of work against dissipative forces requires us to examine instantaneous motion to calculate the associated average power, but the path independence of work to change mechanical energy makes the associated average power independent of such an examination.

### 4.2 Kinetic energy

To discuss the effects of mechanical energy, let us consider a bicycle-cyclist system whose centre-of-mass, at a given instant, moves with speed  $V_1$  along the black line whose curvature is  $R_1$ . Neglecting

the kinetic energy of the rotating wheels, we consider the kinetic energy of the system due to the translational motion of the centre of mass,

$$K = \frac{1}{2} m V^2 .$$

A bicycle-cyclist system is not purely mechanical; in addition to kinetic and potential energy, the system possesses internal energy in the form of the cyclist's chemical energy. When the cyclist speeds up, internal energy is converted into kinetic. However, the converse is not true: when the cyclist slows down, kinetic energy is not converted into internal. Thus, to determine the work the cyclist does to change kinetic energy, we should consider only the increases. If the centre-of-mass speed increases monotonically from  $V_1$  to  $V_2$ , the work done is the increase in kinetic energy,

$$\Delta K = \frac{1}{2} m (V_2^2 - V_1^2) .$$

The stipulation of a monotonic increase is needed due to the nonmechanical nature of the system, with the cyclist doing positive work—with an associated decrease in internal energy—when speeding up, but not doing negative work—with an associated increase in internal energy—when slowing down.

In the case of a constant centre-of-mass speed,  $\Delta K = 0$ . Otherwise, for instance, in the case of a constant black-line speed (e.g., Bos et al., 2021, Appendix A, Figure A.1), the increase of  $V$  occurs twice per lap, upon exiting a curve; hence, the corresponding increase in kinetic energy is  $\Delta K = m (V_2^2 - V_1^2)$ . The average power, per lap, required for this increase is

$$P_K = \frac{1}{1 - \lambda} \frac{\Delta K}{t_\odot} ,$$

where  $t_\odot$  stands for the laptime. Since, for a constant centre-of-mass speed,  $\Delta K = 0$ , no power is expended to increase kinetic energy,  $P_K = 0$ .

### 4.3 Potential energy

Let us determine the work—and, hence, average power, per lap—performed by a cyclist to change the potential energy,

$$U = m g h \cos \vartheta .$$

Since we assume a model in which the cyclist is instantaneously in rotational equilibrium about the black line, only the increase of the centre-of-mass height is relevant for calculating the increase in potential energy, and so for obtaining the average power required for the increase. Since the lean angle,  $\vartheta$ , depends on the centre-of-mass speed,  $V$ , as well as on the radius of curvature,  $R$ , of the black line,  $\vartheta$ —and therefore the height of the centre of mass—changes if either  $V$  or  $R$  changes. The work done is the increase in potential energy resulting from a monotonic decrease in the lean angle from  $\vartheta_1$  to  $\vartheta_2$ ,

$$\Delta U = m g h (\cos \vartheta_2 - \cos \vartheta_1) .$$

In the case of a constant centre-of-mass speed, as well as of constant black-line speed,

$$\Delta U = 2 m g h (\cos \vartheta_2 - \cos \vartheta_1) ,$$

since—in either case—the bicycle-cyclist system straightens twice per lap, upon exiting a curve. The average power required for this increase of potential energy is

$$P_U = \frac{1}{1 - \lambda} \frac{\Delta U}{t_\odot} . \tag{23}$$

The same considerations—due to the nonmechanical nature of the system—apply to the work done to change potential energy as to that done to change kinetic energy. The cyclist does positive work—with an associated decrease in internal energy—when straightening up, but not negative work—with an associated increase in internal energy—when leaning into the turn.

As stated in Section 4.1, while we neglect the vertical motion of the centre of mass to calculate, with reasonable accuracy, the power expended against dissipative forces, this approach cannot capture the changes in the cyclist’s potential energy along the transition curves. Instead, herein, we calculate these changes starting from the assumption of instantaneous rotational equilibrium and the resulting decrease in lean angle while exiting a turn. Viewed from the noninertial reference frame of a cyclist following a curved trajectory, the torque causing the lean angle to decrease and potential energy to increase is the fictitious centrifugal torque. This torque arises from the speed of the cyclist, which is in turn the result of the power expended on pedaling. Therefore it follows that the increase in potential energy is subject to the same drivetrain losses as the power expended against dissipative forces and to increase kinetic energy; hence, the presence of  $\lambda$  in expression (23).

Returning to the first paragraph of Section 4.1, we conclude that the changes in potential energy discussed herein are different from the changes associated with hills. When climbing a hill, a cyclist does work to increase potential energy. When descending, at least a portion of that energy is converted into kinetic energy of forward motion. This is not the case with the work the cyclist does to straighten up. When the cyclist leans, potential energy is not converted into kinetic energy of forward motion.

## 5 Constant centre-of-mass speed

In accordance with expression (14), let us find the values of  $P$  at discrete points of the black line, under the assumption of a constant centre-of-mass speed,  $V$ . Stating expression (22), as

$$v = V \frac{R}{R - h \sin \vartheta},$$

we write expression (14) as

$$P = \frac{V}{1 - \lambda} \left\{ \frac{1}{2} C_d A \rho V^2 + \left( C_{rr} m g (\sin \theta \tan \vartheta + \cos \theta) \cos \theta + C_{sr} \left| m g \frac{\sin(\theta - \vartheta)}{\cos \vartheta} \right| \sin \theta \right) \frac{R}{R - h \sin \vartheta} \right\}. \quad (24)$$

Equation (21), namely,

$$\vartheta = \arctan \frac{V^2}{g(R - h \sin \vartheta)},$$

can be solved for  $\vartheta$ —to be used in expression (24)—given  $V$ ,  $g$ ,  $R$ ,  $h$ ; along the straights,  $R = \infty$  and, hence,  $\vartheta = 0$ ; along the circular arcs,  $R$  is constant, and so is  $\vartheta$ ; along transition curves, the radius of curvature changes monotonically, and so does  $\vartheta$ . Along these curves, the radii are given by solutions of equations discussed in Section 2.1 or in Section 2.2.

The values of  $\theta$  are given— at discrete points— from expression (11), namely,

$$\theta(s) = 28.5 - 15.5 \cos \left( \frac{4\pi}{S} s \right).$$

The values of the bicycle-cyclist system,  $h$ ,  $m$ ,  $C_d A$ ,  $C_{rr}$ ,  $C_{sr}$  and  $\lambda$ , are provided, and so are the external conditions,  $g$  and  $\rho$ .

Under the assumption of a constant centre-of-mass speed,  $V$ , there is no power used to increase the kinetic energy, only the power,  $P_U$ , used to increase the potential energy. The latter is obtained by expression (23), where the pertinent values of  $\vartheta$  for that expression are taken from model (24).

## 6 Numerical example

To examine the model, including effects of modifications in its input parameters as well as error propagation, let us consider the following values. An Hour Record of 57500 m, which corresponds to an average laptime of 15.6522 s and the average black-line speed of  $v = 15.9776\text{m/s}$ . A bicycle-cyclist mass of  $m = 90\text{ kg}$ , a surrounding temperature of  $T = 27^\circ\text{C}$ , altitude of 105 m, which correspond to Montichiari, Brescia, Italy; hence, acceleration due to gravity of  $g = 9.8063\text{ m/s}^2$ , air density of  $\rho = 1.1618\text{ kg/m}^3$ . Let us assume  $h = 1.2\text{ m}$ ,  $C_dA = 0.19\text{ m}^2$ ,  $C_{rr} = 0.0015$ ,  $C_{sr} = 0.0025$ ,  $\lambda = 0.015$ .

The required average power—under the assumption of a constant centre-of-mass speed—is  $P = 499.6979\text{ W}$ , which is the sum of  $P_F = 454.4068\text{ W}$  and  $P_U = 45.2911\text{ W}$ ; 90.9% of power is used to overcome dissipative forces and 9.1% to increase potential energy. The corresponding centre-of-mass speed is  $V = 15.6269\text{m/s}$ . During each lap, the power,  $P$ , varies by 3.1% and the black-line speed,  $v$ , by 3.9%, which agrees with empirical results for steady efforts.

Also, during each lap, the lean angle varies,  $\vartheta \in [0^\circ, 47.9067^\circ]$ , and hence, for each curve, the centre of mass is raised by  $1.2(\cos(0^\circ) - \cos(47.9067^\circ)) = 0.3956\text{ m}$ . For this Hour Record, which corresponds to 230 laps, the centre of mass is raised by  $2(230)(0.3956\text{ m}) = 181.9760\text{ m}$  in total.

To gain insight into the sensitivity of the model to input parameters, let us consider  $m = 90 \pm 1\text{ kg}$ ,  $T = 27 \pm 1^\circ\text{C}$ ,  $h = 1.20 \pm 0.05\text{ m}$ ,  $C_dA = 0.19 \pm 0.01\text{ m}^2$ ,  $C_{rr} = 0.0015 \pm 0.0005$ ,  $C_{sr} = 0.0025 \pm 0.0005$  and  $\lambda = 0.015 \pm 0.005$ . For the limits that diminish the required power—which are all lower limits, except for  $T$ —we obtain  $P = 463.6691\text{ W}$ . For the limits that increase the required power—which are all upper limits, except for  $T$ —we obtain  $P = 536.3512\text{ W}$ . The greatest effect is due to  $C_dA = 0.19 \pm 0.01\text{ m}^2$ . If we consider this variation only, we obtain  $P = 477.1924\text{ W}$  and  $P = 522.2033\text{ W}$ , respectively.

To gain insight into the stability and to examine the bias of the model, let us consider a Monte Carlo simulation by sampling one million values from continuous uniform distributions of  $m$ ,  $T$ ,  $h$ ,  $C_dA$ ,  $C_{rr}$ ,  $C_{sr}$ ,  $\lambda$ , with up to  $\pm$  one-percent error. For this simulation, illustrated in Figure 8, the sample mean is  $\mu = 499.6995\text{ W}$  and the maximum percentage error is 1.1275%, which means that the error is multiplied by a factor of 11.275. Since  $\mu$  is within 0.0003% of the errorless prediction and the histogram is symmetric about the mean, the model is unbiased. In Figure 9, which illustrates a Monte Carlo simulation of  $C_dA$  only, with up to  $\pm$  one-percent error, the sample mean is  $\mu = 499.6992\text{ W}$  and the maximum percentage error is 0.8558%, which means that the error is multiplied by 8.558. Also herein,  $\mu$  is within 0.0003% of the errorless prediction and the histogram is quite symmetric about the mean. Examining these results and comparing Figures 8 and 9, we see the dominant effect of  $C_dA$  in multiplication of the input errors.

To gain insight into the effect of significantly different input values on the required power, let us consider several modifications.

**Hour Record:** Let the only modification be the reduction of Hour Record to 55100 m. The required average power reduces to  $P = 440.9534\text{ W}$ . Thus, reducing the Hour Record by 4.2% reduces the required power by 11.8%. However, since the relation between power and speed is nonlinear, this ratio is not the same for other values, even though—in general—for a given increase of speed, the proportional increase of the corresponding power is greater (e.g., Danek et al., 2021, Section 4, Figure 11).

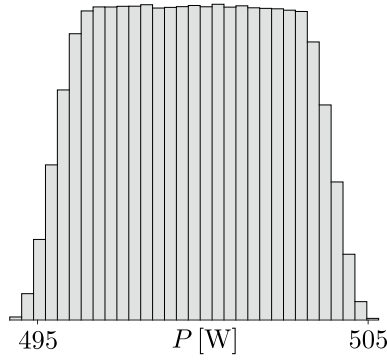


**Figure 8:** Range of required power obtained by one million Monte-Carlo simulations from uniform distributions of  $m$ ,  $T$ ,  $h$ ,  $C_dA$ ,  $C_{rr}$ ,  $C_{sr}$ ,  $\lambda$  with up to  $\pm$  one-percent error

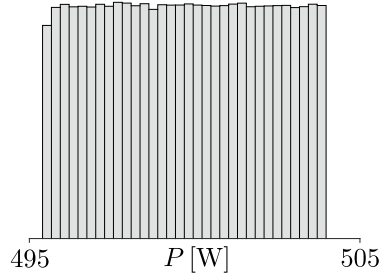


**Figure 9:** Range of required power obtained from one million Monte-Carlo simulations from a uniform distribution of  $C_dA$  with  $\pm$  one-percent error

**Altitude:** Let the only modification be the increase of altitude to 2600 m, which corresponds to Cochabamba, Bolivia. The corresponding adjustments are  $g = 9.7769 \text{ m/s}^2$  and  $\rho = 0.8754 \text{ kg/m}^3$ ; hence, the required average power reduces to  $P = 394.2511 \text{ W}$ , which is a reduction by 21.1%.

**Temperature:** Let the only modification be the reduction of temperature to  $T = 20^\circ\text{C}$ . The corresponding adjustment is  $\rho = 1.1892 \text{ kg/m}^3$ ; hence, the required average power increases to  $P = 509.7835 \text{ W}$ .

**Mass:** Let the only modification be the reduction of mass to  $m = 85 \text{ kg}$ . The required average power reduces to  $P = 495.6926 \text{ W}$ , which is the sum of  $P_F + P_U = 452.9177 \text{ W} + 42.7749 \text{ W}$ . The reduction of  $m$  by 5.6% reduces the required power by 0.8%, which is manifested in reductions of  $P_F$  and  $P_U$  by 0.3% and 5.6%, respectively. In accordance with a formulation in Section 4.3, the reductions of  $m$  and  $P_U$  are equal to one another.

**Centre-of-mass height:** Let the only modification be the reduction of the centre-of-mass height to  $h = 1.1 \text{ m}$ . The corresponding adjustments are  $P_F = 456.7678 \text{ W}$ ,  $P_U = 41.5346 \text{ W}$  and  $V = 15.6556 \text{ m/s}$ ; hence, the required average power decreases to  $P = 498.3023 \text{ W}$ , which reduces the required power by 0.3%; this reduction is a consequence of relations among  $P_F$ ,  $P_U$ ,  $V$  and  $\vartheta$ .

**$C_dA$ :** Let the only modification be the reduction of the air-resistance coefficient to  $C_dA = 0.17 \text{ m}^2$ . The required average power reduces to  $P = 454.6870 \text{ W}$ , which is the sum of  $P_F + P_U = 409.3959 \text{ W} +$

45.2911 W. The reduction of  $C_dA$  by 10.5% reduces the required power by 9.0%,  $P_F$  by 9.9% and no reduction in  $P_U$ .

**Mass and  $C_dA$ :** Let the two modifications be  $m = 85$  kg and  $C_dA = 0.17$ . The required average power is  $P = 450.6817$  W, which is the sum of  $P_F + P_U = 407.9068$  W + 42.7749 W. The reduction in required average power is the sum of reductions due to decreases of  $m$  and  $C_dA$ , 4.0 W + 45.0 W = 49.0 W. In other words, The two modifications reduce the required power by 9.8%, wherein  $P_F$  and  $P_U$  are reduced by 10.2% and 5.6%, respectively.

**Track-inclination asymmetry:** Let the only modification be  $s_0 = 5$ , in expression (12). The required average power is  $P = 499.7391$  W, which is a reduction of less than 0.0%.

**Euler spiral:** Let the only modification be the  $C^2$ , as opposed to  $C^3$ , transition curve. The required average power is  $P = 499.7962$  W, which is a reduction of less than 0.0%.

## 7 Comparison to Fitzgerald et al. (2021)

Let us compare model (14) to Fitzgerald et al. (2021, expression (24)), which—expressed in our notation—is

$$P'_F = \frac{1}{1-\lambda} \left\{ \frac{1}{2} C_dA \rho V^3 + \left( C_{rr} m g \frac{\cos(\vartheta - \theta)}{\cos \vartheta} + C_{rr} \mu_s m g \frac{\cos(\vartheta - \theta)}{\cos \vartheta} |\vartheta - \theta| \right) v \right\}; \quad (25)$$

it omits changes in potential and kinetic energy, but encompasses the dominant resistive forces for steady riding. Model (25) differs from model (14) by using  $\mu_s$ , which is a scrubbing resistance (e.g., Lukes et al. (2012)) associated with the assumption of a slight shifting of the handlebars to avoid lateral slipping down the banked track, as opposed to  $C_{sr}$ , the coefficient of lateral friction. Both models assume that the bicycle-cyclist system follows the black line. Notably, the same restriction is made by Fitton and Symons (2018) to validate their model, even though their initial formulation includes deviations of the wheels from that line.

For the comparison, we use input parameters specified by Fitzgerald et al. (2021, Section 3). For the cyclist,  $h = 1$  m,  $m = 75$  kg,  $C_dA = 0.2$  m<sup>2</sup>,  $C_{rr} = 0.002$ ,  $\mu_s = 0.4125$ /rad,  $\lambda = 0.02$ . For the environmental conditions,  $g = 9.81$  m/s<sup>2</sup>,  $\rho = 1.2$  kg/m<sup>3</sup>. For the velodrome, the length of the track is  $S = 250$  m, the turn radius is  $R = 23.1950$  m, the length of the transition is  $b = 24.9$  m, and the bank angle (Fitzgerald et al. (2021, eq. (19))) is

$$\theta(s) = \left( \frac{\theta_{\max} - \theta_{\min}}{2} \right) \sin \left( \frac{4\pi}{S} s - \frac{\pi}{2} \right) + \frac{\theta_{\max} + \theta_{\min}}{2},$$

where  $\theta_{\min} = 13^\circ$  and  $\theta_{\max} = 43^\circ$ . Using the expressions in Section 2.1, the respective values of the remainder of the quarter circular arc, the half-length of the straight, and the Euler spiral coefficient are

$$c = \frac{\pi R - b}{2} = 23.9846 \text{ m}, \quad a = \frac{S}{4} - b - c = 13.6154 \text{ m}, \quad A = \frac{1}{Rb} = 0.001731 \text{ m}^{-2}.$$

In a manner consistent with our approach, Fitzgerald et al. (2021) specify the instantaneous lean angle and centre-of-mass speed agreeing with expressions (21) and (22)—the numerical experiments



assume a steady ride with  $V = 16$  m/s, which corresponds to  $v = 16.2890$  m/s and, hence,  $t_{\cup} = 15.3511$  s. Using these values, together with  $C_{sr} = 0.0025$ , we compare the models to obtain

$$P_F = 531.2604 \text{ W} \quad \text{and} \quad P'_F = 534.7769 \text{ W}. \quad (26)$$

Hence, our power to overcome dissipative forces is consistent with Fitzgerald et al. (2021) to within one percent:  $100(|P_F - P'_F|/P'_F) = 0.6576\%$ , in spite of a different formulation of lateral forces. Also, for either model, during a lap, the power varies by 2.56% and 2.85%, respectively, which agrees with the assumption of a steady ride.

However, as discussed in Section 4, a velodrome model requires considerations of not only dissipative but also conservative forces. Herein, for either model,  $P_U = 34.0442$  W; hence, we claim that—for our and the Fitzgerald et al. (2021) model, and as opposed to values (26)—the required power is 565.3046 W and 568.8212 W, respectively.

## 8 Conclusions

The mathematical model presented in this article offers the basis for a quantitative study of individual time trials on a velodrome. For a given power, the model can be used to predict lap times; also, it can be used to estimate the expended power from the recorded times. In the latter case, which is an inverse problem, the model can be used to infer values of parameters, in particular,  $C_dA$ ,  $C_{rr}$ ,  $C_{sr}$  and  $\lambda$ .

Let us emphasize that our model is phenomenological. It is consistent with—but not derived from—fundamental concepts. Its purpose is to provide quantitative relations between the model parameters and observables. Its key justification is the agreement between measurements and predictions. The relative simplicity of our model—as well as the model by Fitzgerald et al. (2021) and in contrast to Fitton and Symons (2018)—facilitates an empirical examination of specific assumptions. While the accuracy of measurements is insufficient to distinguish between predictions of  $P_F = 531.2604$  W versus  $P'_F = 534.7769$  W, discussed in Section 7, it is possible to obtain empirical evidence for an increase of  $P_U = 34.0442$  W, predicted by our model.

## Acknowledgements

We wish to acknowledge Mehdi Kordi, for information on the track geometry and for measurements, used in Section 2; Elena Patarini, for her graphic support; Roberto Lauciello, for his artistic contribution; Favero Electronics, for inspiring this study by their technological advances of power meters.

## References

- Benham, G. P., Cohen, C., Brunet, E., and Clanet, C. (2020). Brachistochrone on a velodrome. *Proceedings of the Royal Society A*, 476(2238).
- Birkhoff, G. (1950). *Hydrodynamics: A study in logic, fact, and similitude*. Princeton University Press.
- Bos, L., Slawinski, M. A., Slawinski, R. A., and Stanoev, T. (2021). On modelling bicycle power for velodromes: Part II Formulation for individual pursuits. *arXiv*, 2009.01162 [physics.app-ph].
- Danek, T., Slawinski, M. A., and Stanoev, T. (2021). On modelling bicycle power-meter measurements. *arXiv*, 2103.09806 [physics.pop-ph].

- Fitton, B. and Symons, D. (2018). A mathematical model for simulating cycling: applied to track cycling. *Sports Engineering*, 21:409–418.
- Fitzgerald, S., Kelso, R., Grimshaw, P., and Warr, A. (2021). Impact of transition design on the accuracy of velodrome models. *Sports Engineering*, 24(23).
- Lukes, R., Hart, J., and Haake, S. (2012). An analytical model for track cycling. *Proceedings of the Institution of Mechanical Engineers, Part P: Journal of Sports Engineering and Technology*, 226(2):143–151.
- Martin, J. C., Milliken, D. L., Cobb, J. E., McFadden, K. L., and Coggan, A. R. (1998). Validation of a mathematical model for road cycling power. *Journal of Applied Biomechanics*, 14(3):276–291.
- Solarczyk, M. T. (2020). Geometry of cycling track. *Budownictwo i Architektura*, 19(2):111–119; doi: 10.35784/bud-arch.1621.
- Underwood, L. and Jermy, M. (2010). Mathematical model of track cycling: the individual pursuit. *Procedia Engineering*, 2(2):3217–3222.
- Underwood, L. and Jermy, M. (2014). Determining optimal pacing strategy for the track cycling individual pursuit event with a fixed energy mathematical model. *Sports Engineering*, 17:183–196.

## A Air resistance

To formulate summand (14c), we assume that it is proportional to the frontal surface area,  $A$ , and to the pressure,  $p$ , exerted by air on this area,  $F_a \propto pA$ , where  $p = \rho V^2/2$  has a form of kinetic energy and  $V$  is the relative speed of the centre of mass with respect to the air;  $p$  is the energy density per unit volume. We can write this proportionality as

$$F_a = \frac{1}{2} C_d A \rho V^2,$$

where  $C_d$  is a proportionality constant, which is referred to as the drag coefficient.

A more involved justification for summand (14c) is based on dimensional analysis (e.g., Birkhoff, 1950, Chapter 3). We consider the air-resistance force, which is a dependent variable, as an argument of a function, together with the independent variables, to write

$$f(F_a, V, \rho, A, \nu) = 0;$$

herein,  $\nu$  is the viscosity coefficient. Since this function is zero in any system of units, it is possible to express it in terms of dimensionless groups, only.

According to the Buckingham theorem (e.g., Birkhoff, 1950, Chapter 3, Section 4)—since there are five variables and three physical dimensions, namely, mass, time and length—we can express the arguments of  $f$  in terms of two dimensionless groups. There are many possibilities of such groups, all of which lead to equivalent results. A common choice for the two groups is

$$\frac{F_a}{\frac{1}{2} \rho A V^2},$$

which is referred to as the drag coefficient, and

$$\frac{V \sqrt{A}}{\nu},$$

which is referred to as the Reynolds number. Thus, treating physical dimensions as algebraic objects, we can reduce a function of five variables into a function of two variables,

$$g\left(\frac{F_a}{\frac{1}{2}\rho A V^2}, \frac{V\sqrt{A}}{\nu}\right) = 0,$$

which we write as

$$\frac{F_a}{\frac{1}{2}\rho A V^2} = \varphi\left(\frac{V\sqrt{A}}{\nu}\right),$$

where the only unknown is  $F_a$ , and where  $\varphi$  is a function of the Reynolds number. Denoting the right-hand side by  $C_d$ , we write

$$F_a = \frac{1}{2} C_d A \rho V^2,$$

as expected. In view of this derivation,  $C_d$  is not a constant; it is a function of the Reynolds number. In our study, however — within a limited range of speeds —  $C_d$  is treated as a constant. Furthermore, since  $A$  is difficult to estimate, we include it within this constant, and consider  $C_d A$  as a single value, which we denote as  $C_d A$ .

## B Lean angle

In view of Figure 7, the lean angle of a cyclist is

$$\vartheta = \arctan \frac{F_{cp}}{F_g}, \tag{B.1}$$

where the magnitude of the centripetal force is

$$F_{cp} = \frac{m V^2}{r_{\text{CoM}}}, \tag{B.2}$$

and of the force of gravity is  $F_g = m g$ .

To relate  $F_{cp}$  and  $\vartheta$ , we use results (19) and (20) in expression (16), to obtain

$$F_{cp} = N \sin \theta - F_f \cos \theta = m g \tan \vartheta, \tag{B.3}$$

which is tantamount to expression (B.1). Examining expressions (B.2) and (B.4), we see that the lean angle is a function of the centre-of-mass speed and of the radius of curvature for the centre-of-mass trajectory; it is independent of mass or the track inclination.

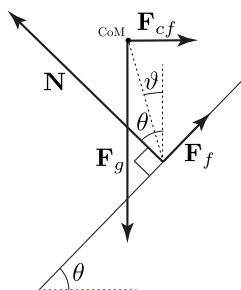


**Figure B1:** Force diagram: Noninertial frame

To relate  $F_{cp}$  and  $\vartheta$ , we use results (19) and (20) in expression (16), to obtain

$$F_{cp} = N \sin \theta - F_f \cos \theta = m g \tan \vartheta, \quad (\text{B.4})$$

which is tantamount to expression (B.1). Examining expressions (B.2) and (B.4), we see that the lean angle is a function of the centre-of-mass speed and of the radius of curvature for the centre-of-mass trajectory; it is independent of mass or the track inclination.

Expressions (B.1) and (B.4) imply that the lean angle,  $\vartheta$ , depends only on the centripetal acceleration of the cyclist's centre of mass and the acceleration of gravity. In other words, the lean angle depends only on the centre-of-mass speed and the radius of curvature of the centre-of-mass trajectory, not on the track inclination,  $\theta$ , even though both the normal force, stated in expression (19), and the frictional force, in expression (20), do depend on track inclination. However, the  $\theta$ -dependence cancels out of the centripetal force, stated in expression (B.4), by a seldom used trigonometric identity.

Given the generality of this result, it would be satisfying to obtain it in a manner that explains it in the context of physics. To this end, let us analyze the situation from inside the noninertial frame of the cyclist. Specifically, we consider the frame comoving with the cyclist around a curve, with the cyclist considered as a point mass. We neglect the additional accelerated motion resulting from the rotation of the cyclist about an axis through the centre of mass.

As illustrated in Figure B1 and in contrast to Figure 7, in this noninertial frame, instead of the forces in the horizontal direction summing to the centripetal force,  $\mathbf{F}_{cp}$ , the forces in this direction, including the fictitious centrifugal force,  $\mathbf{F}_{cf} = -\mathbf{F}_{cp}$ , sum to zero. The centrifugal force must be taken to act at the centre of mass, since otherwise the torque about the centre of mass, stated in expression (17), would be affected.

To proceed, we invoke the vector identity,

$$\sum \boldsymbol{\tau} = \mathbf{R}_{\text{CoM}} \times \sum \mathbf{F} + \sum \boldsymbol{\tau}_{\text{CoM}},$$

where  $\sum \boldsymbol{\tau}$  is the net torque about an arbitrary point,  $\sum \boldsymbol{\tau}_{\text{CoM}}$  is the net torque about the centre of mass,  $\mathbf{R}_{\text{CoM}}$  is the position vector of the centre of mass, and  $\sum \mathbf{F}$  is the net force. From this identity there follows the well-known result that if the net force is zero and the net torque about the centre of mass is zero, the net torque about any other point is also zero. In particular, let us consider the torque about the point of contact of the tires with the surface,

$$\sum \tau_z = h F_g \sin \vartheta - h F_{cf} \sin \left( \frac{\pi}{2} - \vartheta \right) = 0,$$

from which — considering the magnitudes — it follows that

$$\begin{aligned} \tan \vartheta &= \frac{F_{cf}}{F_g} \\ &= \frac{F_{cp}}{F_g}, \end{aligned} \quad (\text{B.5})$$

where expression (B.5) is equivalent to expressions (B.1) and (B.4). Expression (B.5) manifestly holds whether the curve is banked or unbanked.

From inside the noninertial frame of the cyclist, the value of the lean angle obtained for specific values of speed and radius is the one that makes the gravitational torque balance the centrifugal torque. In particular, this condition makes no reference to track inclination.